Clays and Clay Minerals, Vol. 56, No. 1, 90–99, 2008.

NMR SPECTROSCOPY OF NATURALLY OCCURRING SURFACE-ADSORBED FLUORIDE ON GEORGIA KAOLINITE

STACEY G. COCHIARA AND BRIAN L. PHILLIPS*

Center for Environmental Molecular Science, Department of Geosciences, Stony Brook University, Stony Brook, NY 11794-2100, USA

Abstract—Using ^{19}F magic angle spinning (MAS) nuclear magnetic resonance (NMR) spectroscopy, we show that most of the fluoride present in the KGa-1b reference kaolinite from Washington County, Georgia, occurs as a surface-adsorbed species bonded to Al. This surface fluoride can be removed from the <2 μm fraction by acid wash, but is largely retained in the coarse fraction. Correlation of integrated ^{19}F NMR peak intensities with fluoride sorption experiments indicates a bulk F content of ~144 ppm for KGa-1b, of which ~30% substitutes for hydroxyl sites in the mineral structure and the remaining 70% occurs adsorbed on particle surfaces, corresponding to an edge surface fluoride density of ~0.7 F^- nm^{-2}. $^{19}F\{^{27}Al\}$ TRAPDOR (TRAnsfer of Populations in DOuble Resonance) NMR data for the original kaolinite and for products of F^- sorption experiments at pH 4 show that all of the observed ^{19}F signals arise from fluoride bonded to Al atoms. Furthermore, bridging Al-F-Al sites and terminal Al-F give distinctly different TRAPDOR fractions allowing assignment of resolved peaks based on the number of Al in the first coordination sphere. This result was confirmed for fluoride adsorbed to the surface of gibbsite from aqueous suspension. No evidence was found for Si-F-type environments on the kaolinite surfaces.

Key Words—^{19}F NMR, Fluoride, Gibbsite, Kaolinite, Spectroscopy.

INTRODUCTION

The interaction of kaolinite with dissolved fluoride can provide information on kaolinite surface reactivity and the ability of clay minerals to remove fluoride from natural and polluted waters. Application to fundamental surface reactivity is suggested by previous studies showing that measurement of maximum F^- sorption can serve as a probe of the density of reactive surface oxygens of Al and Fe-oxyhydroxides (Perrott *et al.*, 1976; Sigg and Stumm, 1981; Davis and Kent, 1990; Vasudevan and Stone, 1998; Nordin *et al.*, 1999; Hiemstra and van Riemsdijk, 2000). The small size, nucleophilic character, and strong affinity for Al and Fe of the fluoride ion allow it to substitute readily for amphoteric hydroxyl and water molecules singly coordinated to surface sites (M-OH,OH_2), thus providing a measure of fluid-accessible reactive surface area. Fluoride is believed to substitute only for surface sites which are labile to exchange with the fluid, the concentration of which controls rates of processes such as dissolution (*e.g.* Rosenqvist and Casey, 2004). For example, the maximum fluoride sorption density on goethite is much larger than for other anions, and approaches structural estimates for the surface site density of singly coordinated oxygen sites (Davis and Kent, 1990; Hiemstra and van Riemsdijk, 2000). Recent ^{19}F NMR studies have shown that dissolved fluoride can also substitute for bridging hydroxyls (Al-OH-Al) on large dissolved Al polymers (Yu *et al.*, 2003) and on Al-oxyhydroxide surfaces (Nordin *et al.*, 1999), where the presence of Al-F-Al sites was clearly tied to increased dissolution rate. Substitution of fluoride for bridging hydroxyl sites was also inferred to occur on goethite surfaces in the fluoride sorption study of Hiemstra and van Riemsdijk (2000). These results suggest that adsorbed fluoride density could exceed that of available singly coordinated sites if significant substitution also occurs at labile bridging sites, such as at particle steps and edges.

As a model system, the 1:1 layered aluminosilicate structure of kaolinite represents an incremental increase in complexity of a variable-charge mineral surface from the chemically simpler, layered Al and Fe oxyhydroxides studied previously. It is generally recognized that the variable-charge surface of stoichiometric kaolinite is heterogeneous (Sposito, 1984; Huertas *et al*., 1998; Brady *et al*., 1996), in the simplest view containing siloxane top plane, Al-hydroxide bottom plane, and lateral edge surfaces composed of silanol and aluminol groups. The siloxane and Al-hydroxide basal surfaces are unreactive at near-neutral pH, so that the reactivity of kaolinite can be related to the specific edge surface area and the distribution of reactive sites at these edges. This view is reinforced by the low concentration of impurities and non-swelling nature of kaolinite. A motivation of the present study is to determine whether distinct surface sites can be resolved by ^{19}F nuclear magnetic resonance (NMR) spectroscopy of kaolinite reacted with fluoride-containing solutions.

* E-mail address of corresponding author:
brian.phillips@stonybrook.edu
DOI: 10.1346/CCMN.2008.0560108

The interaction of dissolved fluoride with kaolinite also has specific relevance in areas of environmental chemistry. Although fluoride is an essential micronutrient and is added to drinking water to promote dental health, excess exposure to fluoride causes fluorosis, leading to decay of bones and teeth (*e.g.* Meenakshi and Maheshwari, 2006). The gap between recommended fluoride concentrations for potable water and those considered unhealthy is small and spans the range of naturally occurring fluoride concentrations in surface waters and groundwater (Edmunds and Smedley, 2005). Pollutive sources of fluoride can be important in some areas and include by-products of many industrial processes, such as electroplating, manufacture of semiconductors, steels, aluminum, and glass, and preparation of phosphate fertilizers. In addition to its inherent toxicity at high concentration, large fluoride concentrations can increase mobility of metals by increasing the dissolution rates of minerals (Wolff-Boenisch *et al.*, 2004; Nordin *et al.*, 1999; Kau *et al.*, 1997; Zutic and Stumm, 1984; Pulfer *et al.*, 1984) and metal solubility through the formation of strong complexes, especially with Al and Fe.

For these reasons, several studies of fluoride sorption have been reported specifically for kaolinite (Bower and Hatcher, 1967; Perrott *et al.*, 1976; Bar-Yosef *et al.*, 1988; Weerasooriya *et al*., 1998; Kau *et al.*, 1998; Weerasooriya and Wickramarathna, 1999; Agarwal e*t al.*, 2002). These studies have established that fluoride is sorbed strongly by reactions at the kaolinite surface, that sorption increases with decreasing pH, and that fluoride sorption results in release of hydroxyl ion from the mineral surface. For kaolinite, sorption is strongest near pH 4−5, but is negligible above pH 8.5 (Bar-Yosef *et al.*, 1988). Modeling fluoride sorption by kaolinite has generally required Freundlich or competitive Langmuir isotherms, suggesting the presence of a distribution of heterogeneous reaction sites. For example, Weerasooriya *et al.* (1998) modeled kaolinite surface complexation of fluoride over a wide pH range, from 4 to 10, using a triple-layer model with two possible sorption sites, which were interpreted to be $\equiv$SiOH and $\equiv$AlOH groups on particle edges. At the highest fluoride concentrations (0.1 to 1 mM F^-) only a single reaction site, attributed to $\equiv$AlOH, was needed to model the behavior observed in macroscopic batch experiments, whereas adsorption at both types of sites was required at lower concentrations. These results are based only on the removal of dissolved fluoride from the fluid; application of spectroscopic methods could serve to confirm assignments for sorption sites and quantify changes in F^- distribution with loading.

Previous ^{19}F NMR studies have shown that this technique can resolve distinct fluoride environments in various natural and synthetic layered silicates (Huve *et al.*, 1992; Labouriau *et al.*, 1995) and related Al-oxyhydroxides (Nordin *et al.*, 1999). Huve *et al.* (1992) observed very well resolved ^{19}F NMR spectra for a series of 2:1 layered silicates, which showed four distinct sets of peaks that correspond to different combinations of octahedral cations bonded to F. These peaks could be assigned to F^- bonded to two Al in dioctahedral sheets, to one Al and one Mg in dioctahedral sheets, F^- bonded to three Mg in trioctahedral sheets, and to two Mg and one Li in trioctahedral sheets. Labouriau *et al.* (1995) confirmed these results for additional 2:1 dioctahedral and trioctahedral minerals, and found that the ^{19}F NMR peak position for 1:1 dioctahedral clay minerals was very similar to that for pyrophyllite and muscovite, all of which should have F^- mostly bonded to two octahedral Al (Al-F-Al). This result suggests that the ^{19}F NMR peak position depends mostly on the nature of the octahedral cations in its first coordination sphere. The absence of similar Al-F-Al peaks in montmorillonite samples indicated that the F is not randomly distributed, but is preferentially associated with Mg ions in the octahedral sheet. Nordin *et al.* (1999) used ^{19}F NMR to study fluoride sorption by bayerite (β-$Al(OH)_3$) and boehmite (γ-AlOOH) surfaces. At the lowest fluoride surface loading, the NMR spectra are dominated by a peak assigned to terminal (Al-F) sites on particle edges. At higher loading, an additional smaller peak was observed at nearly the same peak position as reported by Huve *et al.* (1992) and Labouriau *et al.* (1995) for fluoride occupying the hydroxyl site in dioctahedral layered silicates. On that basis, the second peak for surface-adsorbed F^- was assigned to fluoride substitution at bridging hydroxyl sites on particle surfaces, forming bridging Al-F-Al sties. The results of these studies indicate that solid-state ^{19}F NMR spectroscopy is useful for determining the fluoride distribution in layered silicates and potentially for F^- adsorbed on their surfaces as well.

In the course of investigating F^- sorption by kaolinite using similar ^{19}F NMR methods, we have found that most of the F^- present in the KGa-1b reference material (Source Clays Repository of The Clay Minerals Society) occurs bonded to Al on the particle surfaces. A ^{19}F NMR spectroscopic study of this surface-adsorbed F^- is presented here. We show that this surface fluoride is mobilized upon suspension in strong acid, is nearly completely removed from the <2 μm fraction, but is retained by the coarse fraction. These results emphasize that natural kaolinite should be pretreated to remove surface-adsorbed fluoride prior to investigations that involve kaolinite surface chemistry.

MATERIALS AND METHODS

Sample materials

The kaolinite samples used in this study were derived from the standard reference material obtained from The Clay Minerals Society Source Clays Repository, denoted as KGa-1b, from Washington County, Georgia. Initial

size fractionation included acid treatment (to pH $\approx$2.1) to remove any carbonate fraction, followed by suspension in basic solution (pH 9) to disperse the particles. The pH of the suspensions was adjusted by additions of 0.1 M HCl and NaOH and measured with a ThermOrion Ross pH electrode that was calibrated on the activity scale. The suspensions were rinsed with deionized water between the acid wash and the particle dispersal. The <2 μm size fraction was isolated by differential settling in a centrifuge. All samples were rinsed in deionized water, decanted, then air-dried prior to NMR analysis. The Brunauer-Emmett-Teller (BET)-measured surface area of the <2 μm fraction was 16.3 m^2g^{-1}, whereas that for the as-received KGa-1b is slightly less, 15 m^2 g^{-1}. Scanning electron microscopy (SEM) back-scatter detector images indicated that the particles in the <2 μm fraction are pseudohexagonal plates with diameters ranging from ~100 to 500 nm.

Fluoride sorption experiments were undertaken on 2.3 g L^{-1} suspensions in 0.1 M CsCl background electrolyte, using a sealed thermo-jacketed reaction vessel and N_2 atmosphere to exclude CO_2. The CsCl was chosen in order to suppress precipitation of Na-aluminofluoride phases such as cryolite. Constant pH was maintained automatically by a Metrohm model 718 titrimeter operating in STAT mode. A calibrated Brinkmann fluoride ion selective electrode (ISE) was used to measure free fluoride concentration. Aliquots of 10 mM fluoride solution were pipetted manually into the vigorously stirred suspension, which was maintained at 25ºC by a circulating water bath, and the electrode reading taken after it had stabilized, typically requiring 1−2 min. Samples for NMR analysis were prepared under the same conditions used for fluoride sorption experiments, with incremental fluoride additions, until the desired free fluoride activity was reached, as measured by the ISE. The suspension was centrifuged for 10 min at 5000 rpm, and the supernatant filtered through a nylon filter (0.2 μm) and saved for analysis. The solids were rinsed with a small amount of deionized water to remove salt, and air-dried for the NMR experiments.

Total fluoride concentrations were determined with the ISE, using Ricca's Total Ionic Strength Adjustment Buffer (TISAB IV); this has been determined to give the most accurate results for fluoride in solutions (Agarwal *et al.*, 2002). Aliquots of the TISAB were added to equal volumes of sample, and the concentration of total fluoride was measured using the fluoride ISE. The amount of fluoride contained in dissolved aluminofluoride complexes was obtained by subtracting the concentration of free fluoride (ISE-detected) from total dissolved fluoride. The concentrations of aluminum and silicon in solution were determined by direct-coupled plasma atomic emission spectrometry (DCP-AES), and were compared to standards of 1−10 ppm Al and Si. All samples were analyzed twice for reproducibility.

The gibbsite sample used was described in detail by Rosenqvist *et al.* (2002). The particles were monodisperse and averaged 209 nm in diameter and 49 nm thick. The BET-measured surface area of the particles was 19.6 m^2/g, which agrees well with the geometrically calculated surface area of 25 m^2/g. Fluoride was added to a suspension of the gibbsite in a 0.1 M CsCl background electrolyte at pH 5 until the final free fluoride concentration in solution was ~0.1 mM.

Solid-state NMR spectroscopy

Solid-state ^{19}F-NMR experiments were conducted using a Varian InfinityPlus NMR spectrometer operating at 470.18 MHz for ^{19}F and 130.23 MHz for ^{27}Al. Samples were spun in 4 mm or 3.2 mm (o.d.) rotors. Both probe assemblies are configured for very low ^{19}F background signal; empty rotors yield no detectable signal after several days of acquisition. The ^{19}F-NMR spectra were taken with single pulse excitation, generally using 4 μs pulses (π = 8 μs) and relaxation delays of 0.5 s. Some spectra were taken at longer relaxation delays (10−20 s) from which a correction factor was obtained to compensate for partial saturation of the signal from internal fluoride. The adsorbed F^- ions exhibit a short spin-lattice relaxation time, whereas that for the internal fluoride is longer such that the corresponding signal is underrepresented by a factor of 1.76 at a 0.5 s relaxation delay. The spinning rates were either 17 kHz or 20 kHz. All peak positions are reported relative to $\delta_{F\text{-}19}$ = 0 ppm for $CFCl_3$, *via* an external reference of monofluorobenzene that was referenced at $\delta_{F\text{-}19}$ = −113 ppm.

The ^{19}F{^{27}Al} TRAPDOR experiments employed the pulse sequence developed by Grey and Vega (1995), with interleaved acquisition of the control (spin-echo) and TRAPDOR spectra, which are obtained without and with irradiation at the ^{27}Al frequency during the spin-echo interpulse delay, τ. The samples were spun at 20−22 kHz, and a ^{19}F $\pi/2$ pulse width of 3 μs was used. The ^{27}Al B_1 field was 56 kHz and the delay, τ, was two rotor periods, typically 0.1 ms. Irradiation at the ^{27}Al frequency during τ in the TRAPDOR experiment causes a decrease in intensity relative to the control spectrum for those F atoms bonded to Al atoms.

RESULTS

^{19}F MAS NMR of KGa-1b

The ^{19}F MAS NMR spectrum of the as-received KGa-1b kaolinite (Figure 1a) contains a relatively narrow peak at a chemical shift $\delta_{F\text{-}19}$ = −133 ppm and a broad set of peaks including components at −140 and −147 ppm. Labouriau *et al.* (1995) observed similar narrow ^{19}F NMR peaks near −135 ppm for natural kaolinite samples from other localities, which were assigned to fluoride substituting for hydroxyl as bridging Al-F-Al groups in the octahedral sheet. This assignment agrees with the results of Huve *et al.* (1992), in which

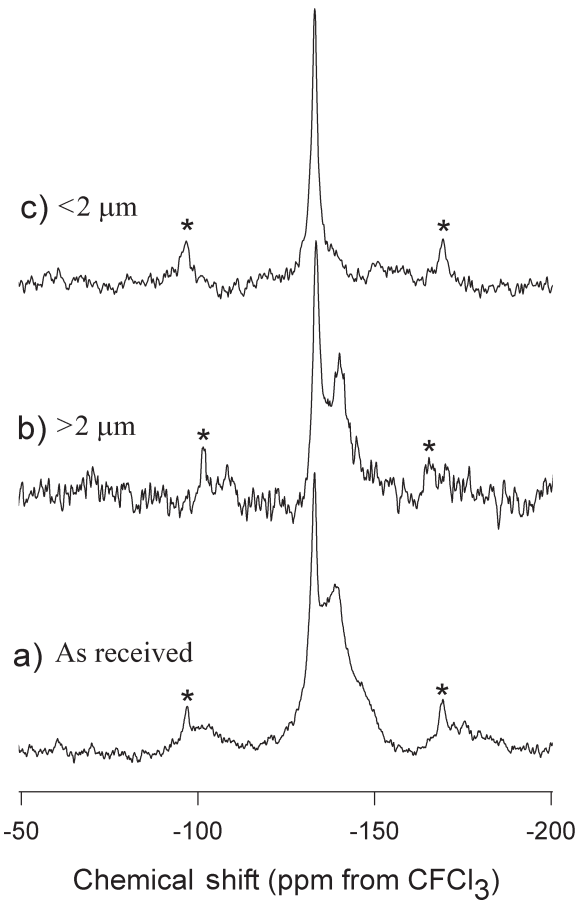

Figure 1. ^{19}F-MAS NMR spectra of KGa-1b kaolinite. (a) As-received material (sample AR); (b) acid-washed and size-fractionated, >2 μm fraction (SF-C); (c) same as (b) but <2 μm fraction (SF-F). Data acquired at 470 MHz, 20 kHz spinning rate, 0.5 s relaxation delay for 20,000 to 120,000 acquisitions. Asterisks denote spinning sideband positions.

^{19}F NMR peaks were observed at −132 and −133 ppm for synthetic dioctahedral 2:1 phyllosilicates. The broad peaks in the −140 to −150 ppm range are not apparent at the slower spinning rates used by Labouriau *et al.* (6 kHz), becoming a broad unresolved peak difficult to distinguish from baseline artifacts. Peaks near −132 and −145 ppm were also observed by Nordin *et al.* (1999) for fluoride adsorbed on bayerite ($Al(OH)_3$) surfaces from aqueous suspensions. For bayerite surfaces, the peak at −145 ppm was assigned to terminal Al-F sites based on structural considerations and the large relative intensity of this peak at low F^- loadings, whereas that at −132 ppm was assigned to bridging Al-F-Al based on the results of Huve *et al.* (1992).

Treatment of the as-received kaolinite with an acid wash and size-fractionation yielded significant changes in the ^{19}F MAS NMR spectra, primarily reduced intensity in the range −140 ppm to −150 ppm (Figure 1b−c). The ^{19}F NMR spectrum of the coarse (>2 μm) fraction (sample SF-C; Figure 1b) showed the narrow peak at −133 ppm and a peak near −140 ppm which corresponds closely to that observed for the as-received sample but with lower relative intensity. The spectrum of the <2 μm fraction (sample SF-F; Figure 1c) contained only a small shoulder at −140 ppm and possibly a weak, broad peak near −160 ppm, in addition to the peak at −133 ppm. These results indicate that the broad peaks at −140 to −150 ppm correspond to the F^-which was largely removed from the fine fraction by the sample treatment, and therefore probably arises from surface-adsorbed species. No change in intensity was observed for the peak at −133 ppm, supporting assignment to F^- substitution on interior hydroxyl sites of the octahedral sheet as proposed previously (Huve *et al.*, 1992; Labouriau *et al.*, 1995).

To determine the fate of the fluoride from the as-received sample, we measured fluoride concentrations in the supernatant sampled after the acid treatment during the size fractionation. The free fluoride concentration in the solution from size fractionation was 0.52 μM, but the total fluoride measured with the TISAB buffer was much greater, 24.43 μM. Therefore, much of the dissolved fluoride in the solution was complexed, probably by Al. For comparison, the total Si in solution was 34 μM and aluminum was 6.4 μM. The results suggest that release of adsorbed fluoride is accompanied by some dissolution, although the presence of dissolved F^- released from the surface could itself enhance the dissolution of kaolinite (Pulfer *et al.*, 1984).

TRAPDOR NMR of KGa-1b and gibbsite

The ^{19}F{^{27}Al} TRAPDOR experiments (Figure 2) indicate that all of the ^{19}F NMR peaks observed for the as-received kaolinite correspond to F bonded to Al. This experiment (Grey and Vega, 1995) compared the signal intensity from a spin-echo experiment performed on the ^{19}F nuclei (S_0) to that of an identical experiment but with irradiation of the ^{27}Al nuclei during the evolution period of the spin-echo, giving signal (S). The presence of ^{27}Al nuclei adjacent to F (within a few Å) reduces the ^{19}F signal intensity in the TRAPDOR spectrum, yielding a TRAPDOR fraction $|1 - S/S_0| > 0$. For sample AR the peak at −133 ppm shows a large TRAPDOR effect, $|1 - S/S_0| = 0.66$, indicating that it corresponds to F closely associated with Al. This result is consistent with assignment of this peak to Al-F-Al environments in the octahedral sheet as described above. The broad peak centered at −140 ppm and shoulder near −147 ppm also show a TRAPDOR effect, indicating that these F are also bonded to Al, but the TRAPDOR fraction, $|1 - S/S_0| = 0.36$, is much smaller than for the peak at −133 ppm. This result suggests assignment of the intensity in the −140 to −150 ppm chemical shift range to terminal Al-F environments on the kaolinite surface. Under similar experimental conditions, bridging sites with two short Al−F distances should exhibit about twice the

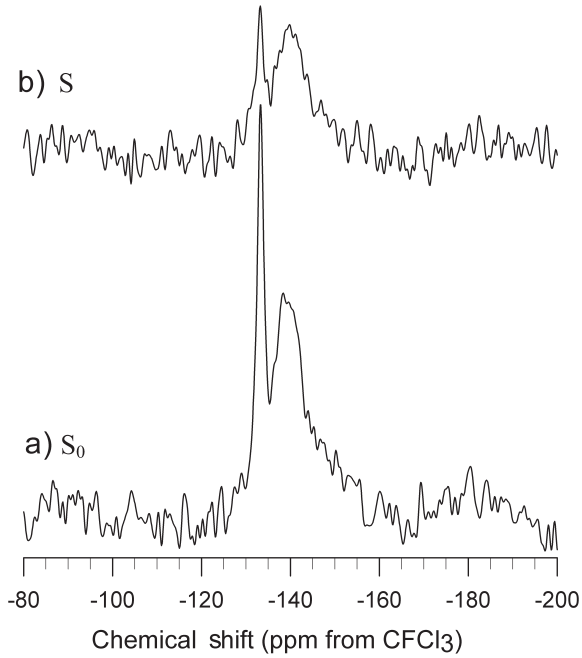

Figure 2. $^{19}F\{^{27}Al\}$ TRAPDOR spectra for the AR KGa-1b kaolinite (untreated). (a) Spin-echo control spectrum (S_0); (b) TRAPDOR spectrum (S) obtained with ^{27}Al irradiation, plotted at the same absolute scaling as for (a). Data acquired at 20 kHz spinning rate and 0.1 ms irradiation period (two rotor periods).

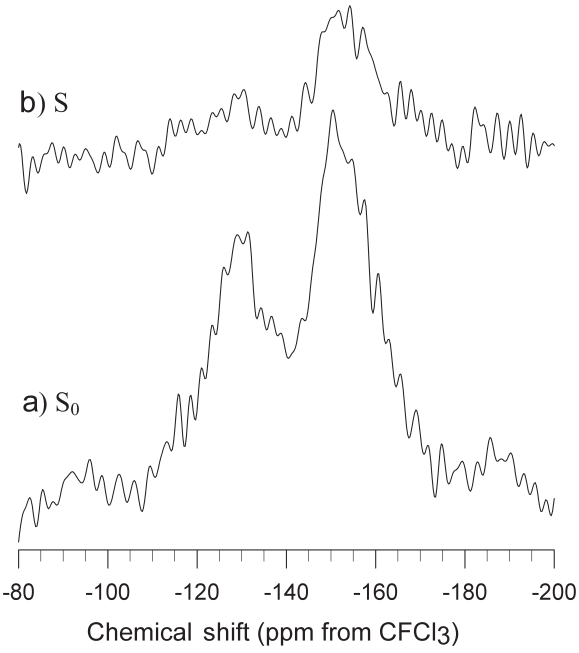

Figure 3. $^{19}F\{^{27}Al\}$ TRAPDOR spectra for gibbsite with surface-adsorbed fluoride added at pH 5. (a) Spin-echo control spectrum (S_0); (b) TRAPDOR spectrum (S) obtained with ^{27}Al irradiation, plotted at the same absolute scaling as for (a). Data acquired at 20 kHz spinning rate and 0.1 ms irradiation period (two rotor periods).

intensity reduction as for terminal sites, which have one short Al−F distance. The TRAPDOR effect depends on the dipolar coupling between ^{27}Al and ^{19}F nuclei, which varies as the sum of the internuclear distances to the inverse third power (*i.e.* $\sum_i [d(F - Al_i)]^{-3}$), so that the Al distribution beyond the first coordination sphere has only a small effect on the $^{19}F\{^{27}Al\}$ TRAPDOR fraction.

For comparison, we also obtained $^{19}F\{^{27}Al\}$ TRAPDOR data for a gibbsite sample with surface-adsorbed fluoride (Figure 3). The spectra contain two peaks, at $\delta_{F\text{-}19} = -129$ ppm and -153 ppm, positions similar to those for kaolinite and for those reported previously for fluoride on bayerite surfaces (Nordin *et al.*, 1999). The difference in TRAPDOR effect for these two peaks is similar to that observed for the kaolinite, with the peak at -129 ppm showing a significantly greater decrease in intensity ($|1 - S/S_0| = 0.80$) than that at -153 ppm ($|1 - S/S_0| = 0.55$). This result indicates assignment of the peaks at -129 ppm and -153 ppm to surface Al-F-Al and terminal Al-F, respectively. Comparison of results for kaolinite with those for gibbsite and other Al-oxyhydroxides (Nordin *et al.*, 1999) indicates that the bridging Al-F-Al sites give chemical shifts near -130 ppm for both internal (kaolinite) and surface (gibbsite, bayerite) sites, and that the terminal Al-F substitution sites on particle surfaces give more negative, though somewhat variable, chemical shifts, with a range from about -140 to -155 ppm.

Fluoride-sorption experiments

Starting with sample SF-F, additional experiments were undertaken to investigate the re-introduction of F^- on the kaolinite surface. These samples were prepared from SF-F at pH 4, above pK_a for HF (3.2) and near the pH reported previously for maximum fluoride sorption by kaolinite (Weerasooriya *et al.*, 1998; Agarwal *et al.*, 2002). A typical sorption isotherm is shown in Figure 4 as a solid line, based on *in situ* potentiometric measurement of free fluoride, along with measurements of sorbed fluoride as the difference between added and total dissolved F^- (free plus complexed) at the preparation conditions for the NMR samples (Figure 4, Table 1). These results show that a significant fraction of the dissolved F^- is complexed at higher loading and invisible to the ISE. Estimated fluoride edge-surface sorption densities (right axis) were calculated from the experimental data using the BET surface area and the results of Bickmore *et al.* (2002) for geometrical edge *vs*. basal surface area for KGa-1b. The sorption data resemble those of previous studies (Kau *et al.*, 1997; Weerasooriya *et al.*, 1998; Agarwal *et al.*, 2002) in that they cannot be fitted with a single-component Langmuir isotherm. However, we do not observe an initial sigmoidal component as reported by Kau *et al*. (1997). Direct comparison with previous studies is difficult because of different methods and materials used; *e.g.* pH was not controlled in previous studies so that sorption

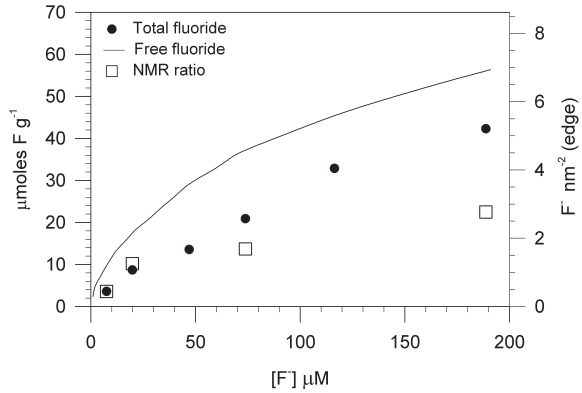

Figure 4. Fluoride sorption isotherm for SF-F kaolinite at pH 4 in 0.1 M CsCl. Solid line calculated from free fluoride concentrations only (ISE-visible), closed symbols calculated from total fluoride concentration (free + complexed) at conditions used to prepare NMR samples SF-1 to SF-5. Open symbols represent total adsorbed fluoride determined from ^{19}F NMR spectra as described in text. Sorption densities are normalized to the BET specific surface area on the right axis assuming 30% edge surface area.

occurred over a range of pH values. Furthermore, we used a CsCl background electrolyte, to suppress precipitation of Na aluminofluorides, and shorter reaction times to minimize dissolution. The apparent F^- sorption density at greater free fluoride concentrations (200 µM) approaches what might be expected for saturation of surface Al sites based on simple crystallographic models (Sposito, 1984).

^{19}F NMR of surface-adsorbed fluoride

At low fluoride loading, the ^{19}F NMR spectrum is dominated by the peak at −133 ppm for interior fluoride, and by a broader peak near −138 ppm (Figure 5b), but also includes a small, narrow peak at −150 ppm. With increasing sorption density, an additional peak near −143 ppm occurs, along with a broad shoulder at

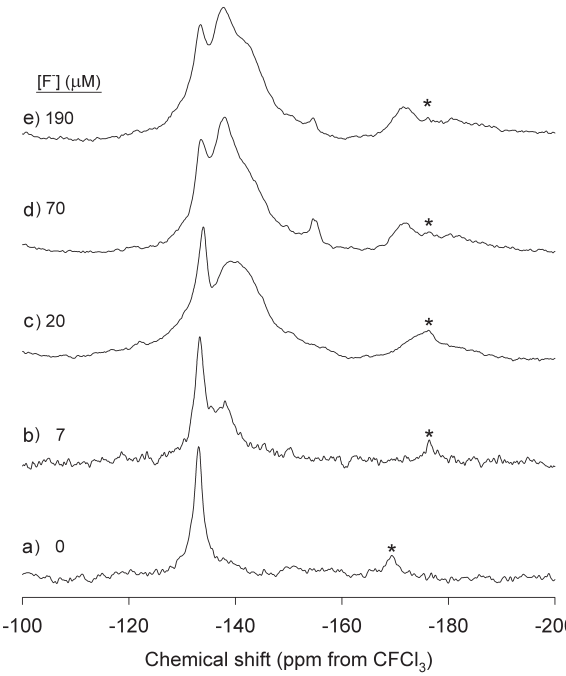

Figure 5. ^{19}F MAS NMR spectra of acid-washed KGa-1b (<2 µm) with increasing F^- sorption density at pH 4 (Figure 4). (a) Sample SF-F, no added F^-; (b) SF-1, 7 µM F^-; (c) SF-2, 20 µM F^-; (d) SF-3, 70 µM F^-; (e) SF-4, 190 µM F^-. Asterisks denote spinning sidebands.

−130 ppm, and a narrow peak at −154 ppm (Figure 5c–e). At the highest F^- concentrations studied, a peak occurs at −172 ppm that can be assigned to crystalline AlF_3 based on this chemical shift (Chupas *et al.*, 2001). In the ^{19}F NMR spectra we did not observe peaks for cryolite or chiolite (−190 ppm; Zeng and Stebbins, 2000) or for rosenbergite ($AlF_3 \cdot H_2O$), which gives a series of narrow peaks from −145 to −160 ppm (Chupas *et al.*, 2003). The small, narrow peak at

Table 1. Samples and preparation conditions for materials used for NMR experiments.

Sample	Starting sample	Preparation	Figures	Sorbed F^- (µmoles g^{-1})
A.R.	KGa-1b	none (as received)	1a, 2	
SF-F	AR	acid wash (pH 2.1) <2 µm fraction	1c, 5a	
SF-C	AR	acid wash (pH 2.1) >2 µm fraction	1b	
SF-1	SF-F	pH 4, 7 µM F^-	5b	3.8
SF-2	SF-F	pH 4, 20 µM F^-	5c	8.7
SF-3	SF-F	pH 4, 70 µM F^-	5d, 6	20.9
SF-4	SF-F	pH 4, 190 µM F^-	5e	42.4
SF-5	SF-F	pH 4, 14 µM F^-		6.5
Gibbs/F	synth. gibbsite	pH 5, 100 µM F^-	3	n.d.

Fluoride concentrations correspond to free (uncomplexed, ISE-visible) fluoride only.
Sorbed F^- calculated from the difference of added and total (free + complexed) fluoride.
n.d.: not determined

−154 ppm observed in some spectra in Figure 5 could not be assigned, and its intensity was too low to allow further investigation by double-resonance methods.

All of the signal from −138 to −151 ppm can be assigned to terminal Al-F sites on the kaolinite surface based on the $^{19}F\{^{27}Al\}$ TRAPDOR results for sample SF-3 (Figure 6). Both the control (S_0) and TRAPDOR spectra (S) can be fitted with the same set of broad peaks (at −130, −138, −143, and −151 ppm) plus a narrow peak at −133 ppm, which, as discussed below, is the minimum number of components needed to fit all the spectra in Figure 5. The TRAPDOR fractions were estimated by fitting both spectra to the same set of peaks (positions and widths), allowing only the intensities to vary in the fit. All of the peaks in the range −138 to −151 ppm exhibit similar TRAPDOR fractions of 0.41±0.07 whereas that obtained for the peaks at −130 and −133 ppm are 0.72±0.05 and 0.74±0.03, respectively. These results are consistent with assignment of F bonded to one (−138 to −151 ppm) or two (−130 and −133 ppm) Al atoms, and indicate that the poorly resolved shoulder near −130 ppm probably arises from F^- substitution on surface bridging sites, which represent only a small fraction of the total adsorbed F^- (<10%). On this basis, we can conclude that fluoride substitution on bridging sites appears to be minor compared to the substitution at terminal sites represented by the peaks at −138 to −151 ppm, and is much less than observed for the Al-oxyhydroxides (*cf.* Figure 3). These data show no evidence of Si-F-type environments, because all portions of the signal exhibit a TRAPDOR effect. Any terminal Si-F sites would appear at the same peak height in Figures 6a and 6b. Although we cannot unambiguously rule out the presence of a small peak for Si-F, such environments cannot account for more than a small fraction of the surface-adsorbed fluoride.

The presence of the peak at −133 ppm, from a constant concentration of intrinsic fluoride substitution in the octahedral sheet, allows quantitative comparison of the amount of surface-adsorbed fluoride among

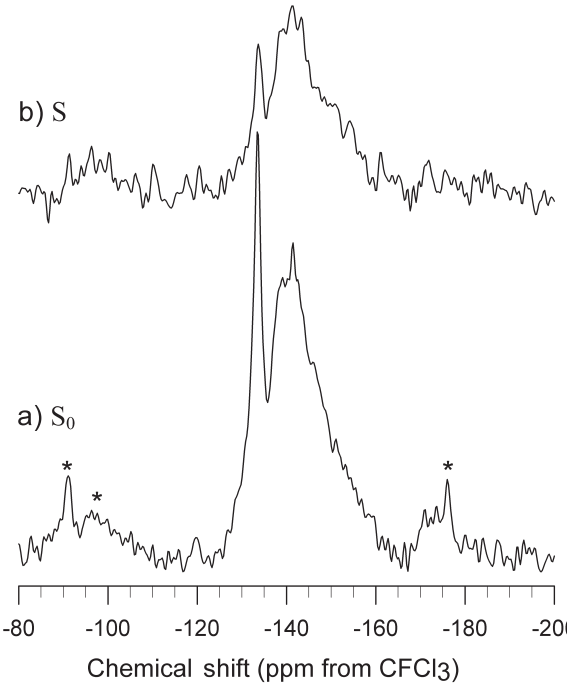

Figure 6. $^{19}F\{^{27}Al\}$ TRAPDOR spectra for kaolinite/fluoride sample SF-3: (a) spin-echo control spectrum (S_0); (b) TRAPDOR spectrum (S) obtained with ^{27}Al irradiation, plotted at the same absolute scaling as for (a). Data acquired at 20 kHz spinning rate and 0.1 ms irradiation period (two rotor periods). Asterisks denote positions of spinning sidebands.

samples. For this purpose, we fitted the ^{19}F NMR spectra to a sum of Gaussian curves that were fixed to the chemical shifts listed in Table 2, plus associated spinning sidebands, allowing variations primarily in peak height with only small, systematic variations in the peak widths. This spectral model corresponds to the minimum number of peaks required to fit all the spectra in Figure 5, and is physical in the sense that changes with sorption density correspond to variation in the populations of a fixed set of adsorption sites. From

Table 2. Integrated relative intensities of peaks fitted to the ^{19}F NMR spectra of as-received KGa-1b kaolinite (AR) and products of kaolinite/F sorption experiments.

Sample	^{19}F chemical shift (ppm)					Ratio
	−130	−133	−138	−143	−151	F_{int}:F_{ads}
SF-1	0.03	0.50	0.41	0.04	0.02	1:1.0
SF-5	0.12	0.29	0.46	0.11	0.03	1:2.5
SF-2	0.10	0.26	0.34	0.25	0.05	1:2.8
SF-3	0.06	0.21	0.52	0.17	0.04	1:3.8
SF-4	0.04	0.14	0.47	0.28	0.07	1:6.3
			−136	−140	−147	
AR	0.04	0.26	0.21	0.35	0.13	1:2.8

The intensity of the peak due to internal F (F_{int}; $\delta_{F\text{-}19}$ = −133 ppm) was adjusted by a factor of 1.76 to account for differential relaxation effects. Small peaks near −120, −154, and −170 (AlF_3) present in some spectra have been omitted. Note that slightly different chemical shifts are observed for adsorbed fluoride of sample AR. Estimated uncertainty is ±0.03 absolute.

comparison of the relative integrated areas for the peak at −133 ppm to the sum of that for other peaks in the spectrum assigned to surface species (−130, and −138 to −151 ppm), we determined the ratio of fluoride on internal (F_{int}) to adsorbed sites (F_{ads}; Table 2), excluding fluoride present in the AlF_3 precipitate. The ratio of adsorbed to internal fluoride is ~1:1 for the sample at smallest fluoride loading (SF-1), and increases to ~6.3:1 for the sample at the greatest loading studied (sample SF-4).

Fitting the spectrum for the AR KGa-1b with a similar model gave a F_{int}:F_{ads} ratio of 1:2.8, but required peak positions that differed from those of the sorption samples (Table 2). We estimate that the internal fluoride peak corresponds to ~38 ppm F (μg F per g kaolinite), by assuming that all of the fluoride missing from the aqueous phase for sample SF-1 (smallest F^- loading) is adsorbed fluoride, and therefore corresponds quantitatively to the sum of the integrated NMR intensities for all the peaks except that at −133 ppm. From the F_{int}:F_{ads} ratio of 1:2.8 for the as-received KGa-1b kaolinite, we estimate that the total (adsorbed + internal) F content is 144 μg g^{-1}. This value is in excellent agreement with the analyzed value of 140 ppm F reported by Thomas *et al.* (1977) for a similar, well crystallized Georgia kaolinite from the Source Clays Repository that appears to have been analyzed for F without any sample treatment. Our results indicate that ~70% of the F content of KGa-1b can be attributed to fluoride adsorbed to the particle surfaces.

An adsorption isotherm can be constructed from the intensities of the NMR spectra and is shown in Figure 4 as open symbols. The values for the density of adsorbed F^- were obtained using the intensity ratios of the peaks for adsorbed to internal fluoride, the estimated internal fluoride content determined above (38 ppm), and the measured BET surface area. These results indicate that the NMR spectra detected only some of the fluoride missing from the solution at greater free-fluoride activity. Resolution of this discrepancy requires further study but could arise from loss of adsorbed fluoride during sample rinsing, loss of a very fine precipitate (*e.g.* AlF_3), or incomplete decomplexation of aqueous aluminofluoride complexes during the total fluoride analysis. The solids recovered appear to contain only small amounts of precipitates, mostly AlF_3.

DISCUSSION

From the isotherm in Figure 4, we estimate that a free-fluoride concentration of ~20 μM is required at pH 4 to yield a surface fluoride density similar to that of the AR KGa-1b (1:2.8 ratio of internal to adsorbed F). This concentration is well within the range for natural waters (Bower and Hatcher, 1967). However, the distribution of surface F^- environments clearly differs between AR KGa-1b and the sample that was derived from SF-F and prepared near these conditions (SF-2), as shown in Table 2. The ratio of internal to total adsorbed F^- for both samples is 1:2.8, but the peak positions of the terminal Al-F are different, with the SF-2 sample giving main peaks at the same positions as for the other sorption samples, −138 and −143 ppm, compared to −136, −140, and −147 for the AR KGa-1b. The different peak positions might reflect different pH or ionic strength conditions at which the F^- adsorption occurred. The ^{19}F NMR chemical shifts are strongly dependent on hydrogen-bond interactions (*e.g.* Liu and Tossell, 2003), so that subtle structural differences could give significant variations in chemical shift. In addition, surface morphology might have been altered by the sample treatment to produce the SF-F starting material for the sorption experiments, which included dissolution of some material.

Our ^{19}F NMR results indicate that several distinct inner-sphere adsorption sites for fluoride occur on the kaolinite surface, including at least three distinct types of terminal Al-F environments, but that only a minor amount of substitution to form bridging Al-F-Al sites occurs. At present, the distinct NMR peaks for surface Al-F cannot be assigned to specific surface structures, beyond the suggestion from previous studies that increased hydrogen bond strength should give more positive chemical shift (*e.g.* Liu and Tossell, 2003). This interpretation is supported by the significantly different ^{19}F NMR chemical shift for singly coordinated Al-F surfaces sites on bayerite (−142 ppm; Nordin *et al.*, 1999) compared with that observed for gibbsite (−153 ppm) in the present study. Both minerals contain only dioctahedral sheets and differ only in the layer stacking. Inspection of possible kaolinite edge surface terminations shows that a large number of distinct terminal sites can be delimited, which differ in the types of anion environments adjacent to the terminal Al−F, including bridging Al-O-Al, bridging Si-O-Al, and terminal Al-OH/OH_2. Furthermore, distinct hydrogen-bond environments might be expected for terminal sites on the basal plane of the octahedral sheet compared to the plane between the tetrahedral and octahedral sheets. In particular, at greater F^- loading, it is possible for more than one F^- to be bonded to the same surface Al, which could also give a different ^{19}F chemical shift as suggested by Fischer *et al.* (2000). However, we do not believe that different numbers of F^- bonded to Al can account for the main peaks, because the resolved peaks have sub-equal intensity at relatively low F loading, and ^{19}F chemical shifts for $AlF_x(OH_{6-x})^{3-x}$ complexes in aqueous solution differ by <1 ppm (*e.g.* Bodor *et al.*, 2000). Also, multiple F^- substitution on the same Al center should give large spinning sidebands from the strong dipolar coupling that would result from the short F−F distance. The relative peak intensities of the first-order spinning sidebands of the sorption samples closely resemble those of the center band, indicating that the

resolved components experience similar dipolar coupling and chemical-shift anisotropy.

From the NMR data the non-Langmuirian nature of fluoride sorption for kaolinite clearly results naturally from heterogeneous distribution of adsorption sites, which can reasonably be expected to exhibit distinct, and possibly correlated, equilibria with aqueous fluoride. In addition to the distinct ^{19}F NMR peaks observed, each peak is relatively broad (*e.g.* compared to that for the internal F), indicating that each of the resolved peaks and shoulders represents a distribution of local chemical environments. Our results support the use of heterogeneous adsorption models for fluoride uptake by kaolinite, using multiple sites. However, we find no evidence for significant participation by Si-F type environments, as proposed by Weerasooriya *et al.* (1998), because all of the adsorbed F^- appears to exhibit ^{27}Al TRAPDOR effects at short irradiation periods. Additional NMR experiments to quantify the distribution of fluoride on kaolinite and its variation with pH and sorption density are currently underway.

Of broader interest, the NMR data presented here show that a large fraction of the fluoride present in the KGa-1b reference kaolinite occurs adsorbed to the particle surfaces, corresponding to >70% of the total F. Assuming that the density of terminal Al-OH/Al-OH_2 sites on kaolinite particle edges is 5.3 nm^{-2} (Sposito, 1984) and that the edges represent 30% of the BET-measured surface area (Bickmore *et al.*, 2002), the total adsorbed F^- estimated from NMR (106 μg F/g kaolinite) corresponds to a density of Al-F on the particle edges of 0.7 nm^{-2}, or ~15% of the available Al-bound terminal sites. This fluoride is released by suspension in strong acid, but at neutral to slightly acidic conditions fluoride might prove difficult to remove owing to its strong affinity for Al. Although the <2 μm fraction appears to be mostly free of surface F^-, the coarse fraction retains a significant fraction of the adsorbed fluoride. This behavior could indicate the presence of internal surfaces in particle aggregates that are inaccessible to the fluid on the time-scale of our sample preparation.

These observations may have some bearing on the results of previous studies that have used this reference material without an acid wash or size-fractionation in the sample preparation. The surface-adsorbed fluoride can be expected to exert some influence on sorption and dissolution rate measurements that might also vary with sample treatment. For example, adsorbed fluoride reverses the polarity of the hydrogen bond donor/acceptor orientation in the surface fluid layer (Hiemstra and van Riemsdijk, 2000). Although we have thus far examined only the KGa-1b reference material, we anticipate that kaolinite from other localities is likely to contain adsorbed fluoride, because the small aqueous F^- concentration needed for significant surface coverage is well within the range for natural waters. Application of standard practices of acid wash and size fractionation should yield a fluoride-free surface, which can be confirmed by ^{19}F MAS/NMR spectroscopy.

ACKNOWLEDGMENTS

We thank Prof. W.H. Casey and Jorgen Rosenqvist for providing the gibbsite sample and for helpful discussion. Improvements to the manuscript resulted from detailed comments by an anonymous reviewer. This work was funded by the US NSF grant numbers EAR 03-10200 and CHE 03-21001 (for instrumentation).

REFERENCES

Agarwal, M., Rai, K., Shrivastav, R., and Dass, S. (2002) A study on fluoride sorption by montmorillonite and kaolinite. *Water Air and Soil Pollution*, **141**, 247–261.

Bar-Yosef, B., Afik, I., and Rosenberg, R. (1988) Fluoride sorption by montmorillonite and kaolinite. *Soil Science*, **145**, 194–200.

Bickmore, B.R., Nagy, K.L., Sandlin, P.E., and Crater, T.S. (2002) Quantifying surface areas of clays by atomic force microscopy. *American Mineralogist*, **87**, 780–783.

Bodor, A., Toth, I., Banyai, I., Szabo, Z., and Hefter, G.T. (2000) ^{19}F NMR study of the equilibria and dynamics of the Al^{3+}/F^- system. *Inorganic Chemistry*, **39**, 2530–2537.

Bower, C.A. and Hatcher, J.T. (1967) Adsorption of fluoride by soils and minerals. *Soil Science*, **103**, 151–155.

Brady, P.V., Cygan, R.T., and Nagy, K.L. (1996) Molecular controls on kaolinite surface charge. *Journal of Colloid and Interface Science*, **183**, 356–364.

Chupas, P.J., Ciraolo, M.F., Hanson, J.C., and Grey, C.P. (2001) In situ X-ray diffraction and solid-state NMR study of the fluorination of γ-Al_2O_3 with HCF_2Cl. *Journal of the American Chemical Society*, **123**, 1694–1702.

Chupas, P.J., Corbin, D.R., Rao, V.N.M., Hanson, J.C., and Grey, C.P. (2003) A combined solid-state NMR and diffraction study of the structures and acidity of fluorinated aluminas: Implications for catalysis. *Journal of Physical Chemistry B*, **107**, 8327–8336.

Davis, J.A. and Kent, D.B. (1990) Surface complexation modeling in aqueous geochemistry. Pp. 177–260 in: *Interface Geochemistry* (M.F. Hochella and A.F. White, editors). Reviews in Mineralogy, **23**, Mineralogical Society of America, Washington, D.C.

Edmunds, W.M., and Smedley, P.L. (2005) Fluoride in natural waters Pp. 301–330 in: *Essentials of Medical Geology: Impacts of the Natural Environment on Public Health* (O. Selinus, editor). Academic Press, New York.

Fischer, L., Harle, V., Kasztelan, S., and de la Caillerie, J.B.D. (2000) Identification of fluorine sites at the surface of fluorinated γ-alumina by two-dimensional MAS NMR. *Solid State Nuclear Magnetic Resonance*, **16**, 85–91.

Grey, C.P. and Vega, A.J. (1995) Determination of the quadrupole coupling constant of the invisible aluminum spins in zeolite HY with ^{1}H/^{27}Al TRAPDOR NMR. *Journal of the American Chemical Society*, **117**, 8232–8242.

Hiemstra, T. and van Riemsdijk, W.H. (2000) Fluoride adsorption on goethite in relation to different types of surface sites. *Journal of Colloid and Interface Science*, **225**, 94–104.

Huertas, F.J., Chou, L., and Wollast, R. (1998) Mechanism of kaolinite dissolution at room temperature and pressure: Part I. surface speciation. *Geochimica et Cosmochimica Acta*, **62**, 417–431.

Huve, L., Delmotte, L., Martin, P., Ledred, R., Baron, J., and Saehr, D. (1992) ^{19}F MAS-NMR study of structural fluorine

in some natural and synthetic 2:1 layer silicates. *Clays and Clay Minerals*, **40**, 186–191.

Kau, P.M.H., Smith, D.W., and Binning, P.J. (1997) The dissolution of kaolin by acidic fluoride wastes. *Soil Science*, **162**, 896–911.

Kau, P.M.H., Smith, D.W., and Binning, P. (1998) Experimental sorption of fluoride by kaolinite and bentonite. *Geoderma*, **84**, 89–108.

Labouriau, A., Kim, Y.W., Chipera, S., Bish, D.L., and Earl, W.L. (1995) A ^{19}F nuclear magnetic resonance study of natural clays. *Clays and Clay Minerals*, **43**, 697–704.

Liu, Y. and Tossell, J. (2003) Possible Al-F bonding environment in fluorine-bearing sodium aluminosilicate glasses: From calculation of ^{19}F NMR shifts. *Journal of Physical Chemistry B*, **107**, 11280–11289.

Meenakshi and Maheshwari, R.C. (2006) Fluoride in drinking water and its removal. *Journal of Hazardous Materials*, **137**, 456–463.

Nordin, J.P., Sullivan, D.J., Phillips, B.L., and Casey, W.H. (1999) Mechanisms for fluoride-promoted dissolution of bayerite [β-$Al(OH)_3$(s)] and boehmite [γ-AlOOH]: ^{19}F-NMR spectroscopy and aqueous surface chemistry. *Geochimica et Cosmochimica Acta*, **63**, 3513–3524.

Perrott, K.W., Smith, B.F.L., and Inkson, R.H.E. (1976) Reaction of fluoride with soils and soil minerals. *Journal of Soil Science*, **27**, 58–67.

Pulfer, K., Schindler, P.W., Westall, J.C., and Grauer, R. (1984) Kinetics and mechanism of dissolution of bayerite (γ-$Al(OH)_3$) in HNO_3-HF solutions at 298.2°K. *Journal of Colloid and Interface Science*, **101**, 554–564.

Rosenqvist, J. and Casey, W.H. (2004) The flux of oxygen from the basal surface of gibbsite (α-$Al(OH)_3$) at equilibrium. *Geochimica et Cosmochimica Acta*, **68**, 3547–3555.

Rosenqvist, J., Persson, P., and Sjoberg, S. (2002) Protonation and charging of nanosized gibbsite (α-$Al(OH)_3$) particles in aqueous suspension. *Langmuir*, **18**, 4598–4604.

Sigg, L. and Stumm, W. (1981) The interaction of anions and weak acids with the hydrous goethite (α-FeOOH) surface. *Colloids and Surfaces*, **2**, 101–117.

Sposito, G. (1984) *The Surface Chemistry of Soils*. Oxford University Press, New York, 234 pp.

Thomas, J., Glass, H.D., White, W.A., and Trandel, R.M. (1977) Fluoride content of clay minerals and argillaceous earth materials. *Clays and Clay Minerals*, **25**, 278–284.

Vasudevan, D. and Stone, A.T. (1998) Adsorption of 4-nitrocatechol, 4-nitro-2-aminophenol, and 4-nitro-1,2-phenylenediamine at the metal (hydr)oxide/water interface: Effect of metal (hydr)oxide properties. *Journal of Colloid and Interface Science*, **202**, 1–19.

Weerasooriya, R. and Wickramarathna, H.U.S. (1999) Modeling anion adsorption on kaolinite. *Journal of Colloid and Interface Science*, **213**, 395–399.

Weerasooriya, R., Wickramarathne, H.U.S., and Dharmagunawardhane, H.A. (1998) Surface complexation modeling of fluoride adsorption onto kaolinite. *Colloids and Surfaces A*, **144**, 267–273.

Wolff-Boenisch, D., Gislason, S.R., and Oelkers, E.H. (2004) The effect of fluoride on the dissolution rates of natural glasses at pH 4 and 25ºC. *Geochimica et Cosmochimica Acta*, **68**, 4571–4582.

Yu, P., Lee, A.P., Phillips, B.L., and Casey, W.H. (2003) Potentiometric and ^{19}F nuclear magnetic resonance spectroscopic study of fluoride substitution in the $GaAl_{12}$ polyoxocation: Implications for aluminum (hydr)oxide mineral surfaces. *Geochimica et Cosmochimica Acta*, **67**, 1065–1080.

Zeng, Q. and Stebbins, J.F. (2000) Fluoride sites in aluminosilicate glasses: High-resolution ^{19}F NMR results. *American Mineralogist*, **85**, 863–867.

Zutic, V. and Stumm, W. (1984) Effect of organic acids and fluoride on the dissolution kinetics of hydrous alumina: A model study using the rotating disk electrode. *Geochimica et Cosmochimica Acta*, **48**, 1493–1503.

(*Received 8 June 2007; revised 1 October 2007; Ms. 0039; A.E. P. Malla*)